



Open Archive Toulouse Archive Ouverte

OATAO is an open access repository that collects the work of Toulouse researchers and makes it freely available over the web where possible

This is an author's version published in: <https://oatao.univ-toulouse.fr/27914>

Official URL :

<https://doi.org/10.1039/d1cp01129d>

To cite this version:

Decosterd, Laura and Topka, Konstantina Christina^{ORCID} and Diallo, Babacar and Samélor, Diane^{ORCID} and Vergnes, Hugues^{ORCID} and Senocq, François^{ORCID} and Caussat, Brigitte^{ORCID} and Vahlas, Constantin^{ORCID} and Menu, Marie-Joëlle^{ORCID} *An innovative GC-MS, NMR and ESR combined, gas-phase investigation during chemical vapor deposition of silicon oxynitrides films from tris(dimethylsilyl)amine.* (2021) *Physical Chemistry Chemical Physics*, 23 (17). 10560-10572. ISSN 1463-9076

Any correspondence concerning this service should be sent to the repository administrator: tech-oatao@listes-diff.inp-toulouse.fr

An innovative GC-MS, NMR and ESR combined, gas-phase investigation during chemical vapor deposition of silicon oxynitrides films from tris(dimethylsilyl)amine†

Laura Decosterd,^a Konstantina Christina Topka,^{bc} Babacar Diallo,^d Diane Samelor,^b Hugues Vergnes,^c François Senocq,^b Brigitte Causat,^c Constantin Vahlas^b and Marie-Joëlle Menu ^{*a}

Tris(dimethylsilyl)amine (TDMSA) is used in the presence of O₂ and NH₃ for the atmospheric pressure chemical vapor deposition (CVD) of conformal, corrosion barrier silicon oxynitride (SiO_xN_y) films at moderate temperature. Plausible decomposition pathways taking place during the process, as well as resulting gas-phase by-products, are investigated by an innovative methodology, coupling solid-state films characteristics with gas phase analysis. Liquid NMR, gas chromatography coupled with mass spectrometry (GC-MS) and electron spin resonance (ESR) allow probing stable compounds and radical intermediate species in the gas phase. At least fifteen by-products are identified, including silanols, siloxanes, disilazanes, silanamines, and mixed siloxane–silanamine molecules, in addition to more usual compounds such as water. The radical dimethylsilane, Me₂HSi•, is noted across all experiments, hinting at the decomposition of the TDMSA precursor. Deposition of SiO_xN_y films occurs even in the absence of NH₃, demonstrating the judicious choice of the silanamine TDMSA as a dual source of nitrogen and silicon. Additionally, the presence of Si–H bonds in the precursor structure allows formation of SiO_xN_y films at temperatures lower than those required by other conventional silazane/silanamine precursors. Addition of NH₃ in the inlet gas supply results in lower carbon impurities in the films. The identified by-products and formulated decomposition and gas-phase reactions provide stimulating insight and understanding of the deposition mechanism of SiO_xN_y films by CVD, offering possibilities for the investigation of representative chemical models and process simulation.

DOI: 10.1039/d1cp01129d

1. Introduction

Silicon oxynitride (SiO_xN_y) films attract a lot of attention¹ due to their remarkable intrinsic and tunable properties, which are in-between those of silica (SiO₂) and silicon nitride (Si₃N₄) films. The atomic network of amorphous SiO_xN_y is denser than that of SiO₂ due to the partial replacement of O anions by higher

coordinated N ones and for this reason such films present better thermal and chemical stability,² superior hardness³ and enhanced anti-corrosion properties.⁴ At the same time, a SiO_xN_y material presents reduced intrinsic mechanical stress, which commonly describes the more rigid Si₃N₄, avoiding thus the emergence of cracks that can be detrimental to product performance.^{5,6} Even at nitrogen concentrations as low as 10 at%, SiO_xN_y films have been reported to reduce buffered HF etching rate and Na⁺ diffusion.⁷ Due to these properties, silicon oxynitride films and coatings have gathered interest for applications in the fields of solar cells,^{8,9} semi-conductors^{10,11} and packaging.²

SiO_xN_y films are deposited by different techniques, however, when dealing with uniform, conformal and micrometer thick films deposited on thermally sensitive and complex substrates with non-line-of-sight geometries, chemical vapor deposition (CVD) is one of the most suitable methods.¹² Silane (SiH₄) or chlorosilanes are often involved as the silicon-providing precursors and are introduced in the CVD process along with

^a CIRIMAT, Université de Toulouse, CNRS, Université Toulouse 3 – Paul Sabatier, 118 Route de Narbonne, 31062 Toulouse Cedex 9, France.

E-mail: menu@chimie.ups-tlse.fr

^b CIRIMAT, Université de Toulouse, CNRS, INP-ENSIACET, 4, Allée Emile Monso, BP-44362, 31030 Toulouse Cedex 4, France

^c LGC, Université de Toulouse, CNRS, INP-ENSIACET, 4, Allée Emile Monso, BP-44362, 31030 Toulouse Cedex 4, France

^d CNRS, Conditions Extrêmes et Matériaux, Haute Température et Irradiation (CEMHTI) UPR 3079, Université d'Orléans, Site Cyclotron, CS 30058 3A Rue de la Férolerie, 45071 Orléans Cedex 2, France

† Electronic supplementary information (ESI) available. See DOI: 10.1039/d1cp01129d

oxidants such as N_2O , NO_2 or O_2 , with ammonia (NH_3) being conventionally used as the nitrogen source. Nonetheless, in thermal CVD processes that lack plasma activation, temperatures higher than $750\text{ }^\circ\text{C}$ are required to obtain oxynitride films.¹³ As such, it becomes evident that the choice of precursor and the inlet gas composition are the key factors that enable thermal CVD of SiO_xN_y films in lower desired temperature windows.

In that context, the presence of Si–H bonds in the precursor is essential for the reduction of the deposition temperature, as these bonds are known to be easily oxidized and have been reported to activate the deposition mechanism and promote film formation.¹⁴ As an example, the case of hexamethyldisilazane ($(CH_3)_3SiNHSi(CH_3)_3$, HMDSz) is noted, a molecule which does not contain Si–H bonds, and for which the lowest reported temperature for deposition of SiN_x or SiO_xN_y films by thermal CVD is $760\text{ }^\circ\text{C}$.¹³ Contrary to HMDSz, upon addition of Si–H bonds in the precursor molecule, deposition temperatures can be effectively decreased, as illustrated through the bis(tertiary-butylamino)silane (BTBAS) precursor, which contains two Si–H bonds and allows the deposition of SiN_x at $600\text{--}675\text{ }^\circ\text{C}$,¹⁵ with temperatures down to $550\text{ }^\circ\text{C}$ also being reported.¹⁶ The presence of additional Si–H bonds is thus expected to decrease the minimum deposition temperature even further.

Other important information that needs to be taken into account during selection of suitable precursor molecules for SiO_xN_y deposition by thermal CVD is the presence of Si–O bonds. Such bonds can impede the incorporation of nitrogen, as reported by Park *et al.*,¹⁷ who studied the deposition of SiO_2 from 3-aminopropylmethyldiethoxysilane (APMDES) at $650\text{ }^\circ\text{C}$ by thermal CVD. The authors noted that no nitrogen was detected in the films despite the high temperature. In the same sense, Vamvakas *et al.*¹⁸ performed thermodynamic calculations for the thermal CVD of SiO_xN_y from tetraethoxysilane (TEOS) mixtures, concluding that incorporation of nitrogen is not possible at temperatures below $930\text{ }^\circ\text{C}$ or $830\text{ }^\circ\text{C}$, in the presence of N_2O or NH_3 gas, respectively, the biggest hindrance being the four oxygen atoms surrounding the Si atom in the precursor molecule. It is therefore suggested that the presence of Si–O bonds is unfavorable when the production of a SiN_x or SiO_xN_y film is desired at moderately low temperatures, and by contrast, a Si–N bond in the starting precursor should be favored. Although the vast majority of thermal CVD processes utilize NH_3 as a nitrogen source, the innate presence of nitrogen in the precursor itself could prove beneficial when high nitrogen contents are targeted.

In light of the above, the present work focuses on the decomposition mechanisms of tris(dimethylsilyl)amine ($N(SiHMe_2)_3$, TDMSA) that is being used by the authors as precursor in the CVD of SiO_xN_y films. TDMSA is selected given the presence of the desired Si–N and Si–H bonds, while avoiding Si–O ones. Compared to conventional precursors used in CVD of Si_3N_4 and SiO_xN_y , such as silane (SiH_4)^{7,8} and dimethyldichlorosilane ($SiCl_2(CH_3)_2$),^{19,20} it presents lower handling risks and by-passes the production of ammonium chloride encountered during deposition using chlorosilanes. However, it is a complex molecule with a large number of

bonds; the silicon atoms are involved in a tertiary amine, from which many plausible decomposition pathways and products are expected. Therefore, gaining insight into the deposition mechanism and understanding the CVD process from this new precursor requires detailed analysis of both the solid and the gas phase.

Gas phase analysis methods implemented in CVD processes is a common, though not trivial tool to access the deposition mechanisms. For example, *in situ* UV spectroscopic or FTIR exhaust-gas studies have been used to establish chemical reaction paths in the CVD of gallium nitride (GaN) films,^{21,22} and gas chromatography coupled with mass-spectrometry (GC-MS) was applied to investigate the thermal decomposition and by-products generation in CVD of titanium nitride (TiN) films.²³ More recent implementations involve *in situ* Raman spectroscopy during thermal decomposition of a tungsten imido complex by aerosol-assisted (AA)CVD,²⁴ or *in situ* optical emission spectroscopy during microwave plasma-enhanced chemical vapor deposition of phosphorus (P) and nitrogen (N) co-doped nanocrystalline diamond.²⁵ Focusing on analogous studies of CVD processes involving silicon-containing precursors, the majority of the reported literature concerns the binary systems SiC, SiO_2 or Si_3N_4 from chlorosilanes, silanes or TEOS. Among them, Zhang *et al.*²⁶ used GC-MS for the characterization of the gas phase during the deposition of SiC from methyltrichlorosilane in the presence of H_2 , identifying HCl and $SiCl_4$ molecules as by-products. In the same context, Arno *et al.*²⁷ used online FT-IR analysis, detecting primarily carboxylic acids and water, among other compounds, during the SiO_2 deposition from TEOS and O_3 . As for Si_3N_4 films, the gas phase characterization and deposition mechanisms from SiH_4 and NH_3 by photo-assisted CVD, or from SiH_2Cl_2 and NH_3 by low-pressure CVD have been investigated by transient mass spectroscopy.^{28,29}

Despite the existing literature for these chemical systems and materials, the gas phase characterization of a ternary SiO_xN_y and *a fortiori* quaternary $SiO_xN_yC_z$ system remains rather unexplored. In this context, Fainer *et al.* investigated gas mixtures of 1,1,3,3-tetramethyldisilazane ($HSi(CH_3)_2NH$, TMDS) with O_2 and N_2 during plasma chemical decomposition for $SiC_xN_yO_z:H$ nanocomposite films.³⁰ Their gas phase characterization by *in situ* optical emission spectroscopy revealed potential formation of volatile products such as methane CH_4 and CO. However, silicon-containing compounds were absent from their study. More generally, the majority of publications on the CVD of SiO_xN_y films focus mostly on their solid phase characterization and report the gas phase inadequately. However, control and consequently modeling, simulation and ultimately optimization of these complex-in-chemistry processes require comprehensive insight in the gas and surface chemistries.³¹ For this reason, a coupled solid and gas phase analysis proves to be useful in determining potential starting precursors and experimental conditions for the formation of functional films at the lowest possible deposition temperature, as well as in formulating kinetic models for eventual process optimization through utilization of computational fluid dynamics simulations.

Given all that has been presented so far, the present work focuses on the gas phase characterization of a TDMSA-O₂-NH₃ and TDMSA-O₂ CVD process operating at atmospheric pressure, by simultaneously combining classical, multiple physico-chemical methods used in molecular chemistry. A new methodology is proposed, involving gas chromatography coupled with mass spectrometry (GC-MS), nuclear magnetic resonance (NMR) and electron spin resonance (ESR) for the analysis of the gaseous effluents. In particular, ESR, commonly applied for the molecular structural characterization of paramagnetic species, can be used for the characterization of the gas phase,³² constituting an innovative approach for the identification of radical species in CVD processes. Thus, the combination of these three analytical techniques enables the identification of the by-products and intermediates involved in the deposition process.

First, we investigate the thermal behavior of the TDMSA precursor in order to determine its lowest decomposition temperature and the chemical nature of the produced by-products. Then, we undertake deposition experiments with and without ammonia, in order to identify the origin of the nitrogen atoms incorporated in the SiO_xN_y films. This parallel investigation of the gas phase alongside the compositional characterization of the deposited thin films by ion beam analysis (IBA) helps in correlating potential changes in the solid phase to the different by-products identified in the gas phase. This simultaneous consideration, for a set of diverse process parameters (temperature, oxygen and ammonia flow rates), and the thickness and composition of the deposited SiO_xN_y films allows proposing a plausible deposition mechanism, which could be utilized for the development of apparent chemical models and simulation.

2. Experimental section

2.1. Materials

Tris(dimethylsilyl)amine (N(SiHMe₂)₃, TDMSA, **14**), 1,1,3,3-tetra-methyl-disiloxane ((Me₂SiH)₂O, TMDSO, **3**), pentamethyl-disiloxane (Me₂SiH)O(SiMe₃), PMDSO, **6**), 1,1,3,3,5,5-hexamethyl-trisiloxane (Me₂Si(OSiHMe₂)₂, HMTSO, **11**), 1,1,3,3-tetramethyl-disilazane ((Me₂SiH)₂NH, TDMSz, **7**), methoxytrimethylsilane (MeOSiMe₃, MeOTMS, **2**) were purchased from ABCR. Trimethylsilanol (Me₃SiOH, **4**), hexamethyltricyclosiloxane ((Me₂SiO)₃, HMCTSO, **12**), potassium bromide (KBr, FT-IR grade), α -(4-pyridyl-1-oxide)-*N*-*tert*-butylnitrone (C₁₀H₁₄N₂O₂, POBN), hexamethyl-disilazane ((Me₃Si)₂NH, HMDSz, **10**), dimethylsulfoxide-d₆ (DMSO-d₆) and toluene were purchased from Sigma-Aldrich. All the products are used as received.

2.2. Silicon oxynitride deposition

The experimental setup has already been presented in a previous work.³³ The exit of the reactor setup was slightly modified as illustrated in Fig. S1 of ESI,[†] to enable the sampling for the three gas phase analyses. Silicon (100) wafers (Neyco, 24 × 32 mm²) are used as substrates. Before being inserted into the reactor,

they were degreased in a succession of three ultrasound bath steps, including: (1) an ultrasound bath using distilled water for 5 min, then rinsed with acetone, (2) an ultrasound bath using acetone (>99%, VWR Chemicals) for 5 min, then rinsed with ethanol, (3) an ultrasound bath using ethanol (99.3%, VWR Chemicals) for 5 min, and finally dried under Ar (99.9999%, Messer) flow. Within the reactor, the substrates were supported vertically by home-made, tubular, stainless steel substrate holders, with a 7 mm deep insertion slot, positioned on the row. Their total length was 450 mm, supporting a maximum of 18 coupons for each run. Across all experiments utilizing various operating conditions, the coupon positioned at 380 mm from the inlet is systematically used to extract information on the average deposition rate and composition in nitrogen and carbon, and compare the values obtained from different experiments.

2.3. Characterizations of the gas phase and of the film composition

Sampling for GC-MS analysis of the gas phase is done using a 1L Tedlar push lock valve PLV sampling bag with Thermogreen LB-2 Septa (Sigma-Aldrich). Analysis is performed with a Trace 1310 gas chromatograph coupled with a TSQ 900 (Agilent Technologies) mass spectrometer (MS), equipped with a TG-5SILMS column (Thermo Scientific, 30 m length, 0.25 mm i.d., 0.25 μ m film thickness). Helium is used as carrier gas with split mode injector, inserted at 250 °C with a flow rate programmed at 1 mL min⁻¹ for 12 min, then increased and held at 3 mL min⁻¹ for 8 min. Column temperature is programmed and held at 25 °C for 10 min, then increased to 140 °C with a 23 °C min⁻¹ ramp, and finally maintained at 140 °C for 5 min. For every analysis, the transfer line to the MS ion source is set to 250 °C and the MS is used in scan mode with a range from 10 to 600 amu. Using this method, the commercially available silane-based by-products are analyzed in order to corroborate assignments. External calibration is applied for TDMSA with the aim to provide decomposition/conversion percentages. For this purpose, four Tedlar bags are filled with TDMSA and N₂ at room temperature, by flowing 0.80, 1.13, 1.40 and 2.00 standard cubic centimeters per minute (scm) of TDMSA through the reactor. Each bag is analyzed 3 times and, for each TDMSA flow rate, the mean surface area of TDMSA is normalized to the N₂ surface area. The derived calibration curve is confirmed by using additional bags filled with 1.70 and 1.55 scm of TDMSA, and comparing the calculated to the experimental values, out of which an error margin of 11% is established. Calibration curve is given in Fig. S2 of ESI.[†]

The NMR analysis of TDMSA precursor is performed in DMSO-d₆ as a solvent on a Bruker Avance II operating at 400 MHz equipped with a TBO probe. For the NMR analysis of the gas phase during deposition, the outlet gas of the reactor is bubbled in a Schlenk tube containing 0.8 mL of DMSO-d₆ (see Fig. S1, ESI[†]). The solution is then transferred to a NMR tube and analyzed using a Bruker Avance III HD spectrometer operating at 500 MHz, equipped with a Prodigy cryoprobe. The full analysis consisted of ¹H, ¹³C Jmod, ²⁹Si spin echo measurements, HSQC ¹H-¹³C, HSQC ¹H-²⁹Si, HMBC and COSY pulse sequences.

Using the same spectrometer, the commercially available by-products were analyzed in order to confirm their assignment.

The ESR analysis of the gas phase is performed using a KBr-POBN pellet. KBr is first desiccated in an oven at 80 °C for 24 h. Then POBN (50 mg, 0.26 mmol) and KBr (330 mg, 2.80 mmol) are mixed and compacted together to form a pellet of 1 cm diameter. The pellet is placed inside the reactor at 78 cm from the inlet, where the local temperature measures 170 °C. After deposition, the pellet is crushed and transferred into two ESR tubes. One is analyzed as is and the other is washed with toluene (2 mL), and the extracted liquid is analyzed. The two analyses are referred to as “solid phase” and “liquid phase” respectively hereinafter. The analysis of the solid and liquid phases is performed by conventional X-band ESR spectroscopy, using a Bruker Elexsys spectrometer equipped with a high-resolution cavity.

Accurate chemical composition data are provided by the use of Ion Beam Analysis (IBA) techniques, Rutherford Backscattering Spectroscopy (RBS), Nuclear Reaction Analysis (NRA) and Elastic Recoil Detection Analysis (ERDA), performed at the Pelletron facility of CEMHTI in Orléans, France. RBS and NRA are performed at a 166° detection angle with 2 MeV α particles for the former. Oxygen, carbon and nitrogen concentrations are measured through the $^{16}\text{O}(d,\alpha_0)^{14}\text{N}$, $^{12}\text{C}(d,p_0)^{13}\text{C}$ and $^{14}\text{N}(d,p_s)^{15}\text{N}$ nuclear reactions, respectively, using incident deuterons of 0.9 MeV. ERDA measurements are performed using a 2.8 MeV alpha beam. For the measurement of hydrogen, the sample is positioned at a 15° grazing incidence angle and the recoiled hydrogen atoms are collected at a scattering angle of 30°. The overall composition of the films is obtained by simulating the RBS, NRA and ERDA acquire spectra using the SIMNRA software. The chemical structure of all identified compounds is generated by Avogadro version 1.20, an open-source molecular builder and visualization tool.³⁴

3. Results and discussion

3.1. Thermal behavior of TDMSA precursor

In order to analyze the thermal decomposition of TDMSA for the adopted operating conditions, constant flows of 2 sccm TDMSA and 4028 sccm N_2 were introduced in the CVD reactor at different temperatures in the range of 580–700 °C and constant total pressure of 730 torr. The adopted protocol is identical to the one of the CVD of films from TDMSA described in Section 2. The gas phase was collected with a sampling bag at the reactor exit for GC-MS analysis. Fig. 1 presents the conversion percent of the precursor after GC-MS quantification. The results are plotted as a function of the maximum temperature existing in the reactor chamber.

At 580 °C, only 10% of the TDMSA introduced in the reactor is decomposed. Increasing the temperature from 580 °C to 650 °C increases the precursor decomposition from 10 to 81%. Further increase of the temperature up to 700 °C does not significantly influence the TDMSA conversion, which increases

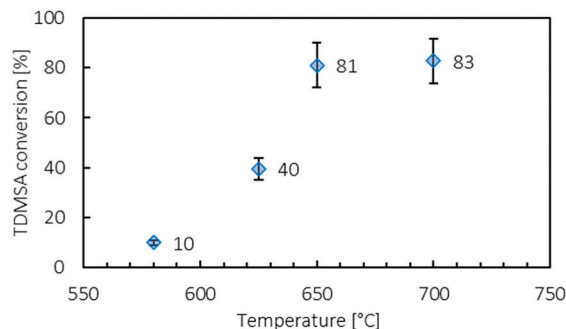


Fig. 1 Evolution of the TDMSA conversion as a function of the temperature.

only slightly from 81 to 83%. The curve reaches a plateau, indicating a possible recombination of the by-products, similarly to what was described by Knolle *et al.*³⁵ with the reformation of the tetramethyldisilazane (TMDSz) during its laser photolysis. Globally, the results indicate that TDMSA does not fully decompose in the probed temperature range, since it is always observed at the exit of the reactor. The study reveals that the decomposition of TDMSA is initiated at around 580 °C and above, with the best compromise between a moderate deposition temperature and a high precursor conversion being 650 °C. As such, the majority of the present study is carried out at this temperature (650 °C), which is significantly lower than the usual 750–900 °C range used for the thermal CVD of SiO_xN_y films.^{13,36} This confirms that the presence of Si–H bonds is favorable for activating the deposition mechanism at lower temperatures, thus decreasing the thermal budget of the process.

Qualitative GC-MS analysis indicated a number of by-products. Among many, $(\text{Me}_2\text{HSi})_2\text{NH}$ (TMDSz) coexists with the starting silanamine precursor at 625 °C. Then in the 650–700 °C range, two supplementary by-products are identified, *i.e.* penta- and hexamethyldisilazanes $(\text{Me}_2\text{SiH})\text{NH}(\text{SiMe}_3)$ (PMDSz) and $(\text{Me}_3\text{Si})_2\text{NH}$ (HMDSz), respectively. The formation of these two compounds only at higher temperature is explained by their molecular structures containing a $-\text{SiMe}_3$ moiety, which requires more energy and additional reaction steps to be formed from this particular starting precursor molecule. It is noted that the fluid dynamics of the current operating configuration can naturally influence the gas phase composition and distribution of identified species under the imposed conditions. However, the length of the reactor (*i.e.* 70 cm), the high dilution of the TDMSA precursor (*i.e.* 2 sccm TDMSA, 4028 sccm N_2 -dilution), the elevated temperatures and the high residence time of the gas (> 1.4 s) allow us to assume a complete mixing.

3.2. Thin films deposition

CVD experiments were carried out at 650 °C using TDMSA and O_2 , with and without ammonia. For all experiments, the TDMSA flow rate and the process pressure were kept constant at 2 sccm and 730 torr, respectively. In order to reach optimal conditions for the deposition of SiO_xN_y , the impact of the NH_3 and O_2 flow rates on the solid and gas phase composition is studied. O_2 flow rate is

Table 1 Detailed deposition conditions and experimental results

	Exp1	Exp2	Exp3	Exp4	Exp5	Exp6
Temperature [°C]	650	650	650	650	650	625
O ₂ flow rate [sccm]	0.6	0.6	0.6	0.3	1.2	0.6
NH ₃ flow rate [sccm]	20	40	—	—	—	—
N at% by IBA	6.3	6.2	5.8	9.8	4.7	4.5
C at% by IBA	8.0	5.9	10.7	20.7	8.0	9.4
Deposition rate [mg min ⁻¹]	1.4×10^{-3}	1.3×10^{-3}	1.6×10^{-3}	1.0×10^{-3}	2.1×10^{-3}	1.4×10^{-3}
TDMSA conversion [%]	81	80	81	86	82	59

varied from 0.3 to 1.2 sccm. Furthermore, for a fixed O₂ flow rate of 0.6 sccm, three parameters are investigated: presence and absence of NH₃ at 650 °C, and deposition at 625 °C in the absence of NH₃. Table 1 presents the experimental conditions (temperature, O₂ and NH₃ flow rates) for each experiment, Exp1 to Exp6, the resulting deposition rates measured by sample weighing and the nitrogen and carbon contents of the SiO_xN_y films determined by IBA, measured on a sample located in the isothermal region of the reactor, positioned at 380 mm from the inlet. The conversion percent of TDMSA, evaluated by quantitative GC-MS, is also included. The by-products identified in the gas phase by coupling GC-MS and NMR analyses are listed in Table 2, together with their respective enumeration and chemical structures where oxygen, nitrogen, carbon and silicon atoms are noted in red, blue, black and green, respectively. Independently of the inlet gas composition, the TDMSA precursor is present in the gaseous effluent, its conversion being around 81% for all experiments conducted at 650 °C. Multiple by-products are observed and fifteen have been identified (Table 2). Identification of the chemical structure of these intermediary compounds gives interesting information to approach the deposition mechanism. Silanols (1, 4, 5 and 9) are observed, which can react directly with the silanol terminated surface sites of the substrate; disiloxanes (3, 6 and 9), trisiloxanes (11 and 12), disilazanes (7, 10 and 13) and even a mixed Si-N-Si-O-Si containing molecule (15) indicate the first steps of the silane condensation. Additional information of interest is the presence of by-products containing trimethylsilyl-substituted molecules (2, 4, 6, 8, and 10) in each of the previously cited families. Identification of such compounds in the gaseous effluent is in agreement with the formation of the SiO_xN_y films, starting from the SiMe₂H substitute molecule. The presence or absence of each of these by-products as a function of the experimental conditions will be discussed in the following sections, together with the respective film composition and deposition rate.




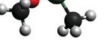
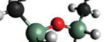

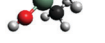
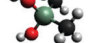
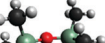

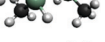
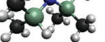
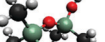

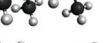
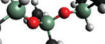
It is noted that the yield of the process was also taken into account, in order to discern the global balance between gas phase and surface reactions. By taking run Exp3 as an example (Table 1), 81% of the supplied precursor is converted, in other words consumed, to produce gaseous by-products in the gas phase and thin film on the solid phase. Additionally, the silicon mass balance was calculated for the same experimental run (Exp3), considering deposition on all solid surfaces (reactor walls, substrate holders, and substrates). Utilizing our available data (film composition, total deposited mass over a specific deposition duration and total TDMSA precursor supply for this

duration), it was calculated that only a maximum of 1% of the silicon supplied in the reactor is converted into solid thin film. Similar values were calculated for all other runs at 650 °C (Exp1 to Exp5). When compared to the relatively high total conversion of the TDMSA precursor (80–86%, Table 1), it becomes evident that gas phase reactions are more prominent than surface reactions. This is in coherence with the large number of silicon-containing by-products identified in the gas phase by GC-MS.

3.2.1. Deposition in presence of NH₃ and O₂. Exp1 was carried out at 650 °C and 0.6 sccm of O₂, in presence of NH₃ serving as nitrogen source. The films are deposited with a 1.4×10^{-3} mg min⁻¹ rate and contain 6.3 at% N and 8.0 at% C. It will be shown, by FT-IR analysis, in a forthcoming publication that carbon is incorporated as CH₃ in the obtained SiO_xN_y films. For these operating conditions, the gas phase contains TDMSA precursor and at least 10 by-products identified (Table 2). These by-products are silanols (1 and 4), siloxanes (3, 6, 9, 11, 12), disilazane (7), silanamine (15) and water. Multiple compounds observed by GC-MS are also encountered in NMR. Interestingly, NMR study allows to evidence the formation of water in this experiment contrary to the GC-MS analysis, for which the identification of H₂O is prevented by its low molecular mass and short retention time.

Fig. 2 presents the ¹H NMR spectrum of the gaseous effluent of Exp1. Due to the variety and multitude of products, analysis is made complex and difficult, requiring various NMR sequences for the accurate assignment of the main products. Despite this complexity, the ¹H NMR spectra (Fig. 2a) systematically show two main zones: one encountered from -0.01 to 0.22 ppm (Fig. 2b) and the other in the 4.60–4.72 ppm range (Fig. 2c). The former is assigned to the methyl resonance of Si-CH₃ moieties, while the latter corresponds to that of hydrogen atoms of Si-H fragments. In the Si-CH₃ zone, singlets are assigned to trimethyl substitutes and doublets, due to the presence of the J_{HH}^3 coupling constant, indicate HSi(CH₃)₂ groups. Even if complete assignment is not possible, compounds 3, 4, 6, 7 and 11 are accurate by comparing with commercial sources. A few additional compounds seem to be hidden underneath other peaks. The low conversion percent and the presence of -SiMe₂ or -SiMe₃ moieties in the molecules in the gas phase are coherent with the formation of a silicon oxynitride SiO_xN_y film containing carbon in aliphatic form. This observation is also in agreement with the results reported by Lee *et al.*³⁷ and Gonzalez-Luna *et al.*,³⁸ indicating that trimethylsilyl derivatives such as HMDSz enhance the carbon content of silicon oxynitride

Table 2 Enumeration and chemical structure of compounds identified by GC-MS and NMR depending on the operating conditions

No.	Chemical structure	Abbreviation	Exp1	Exp2	Exp3	Exp4	Exp5	Exp6
0		—	✓	✓	✓	✓	✓	✓
1		—	✓	✓	✓			
2		MeOTMS			✓	✓	✓	
3		TMDSO	✓	✓	✓	✓	✓	
4		—	✓	✓	✓	✓	✓	✓
5		—			✓			
6		PMDSO	✓		✓			
7		TMDSz	✓		✓	✓	✓	✓
8		PMDSz			✓	✓		
9		—	✓	✓	✓			✓
10		HMDSz				✓		
11		HMTSO	✓	✓	✓	✓	✓	✓
12		HMCTSO	✓		✓	✓	✓	✓
13		—			✓		✓	✓
14		TDMSA	✓	✓	✓	✓	✓	✓
15		—	✓	✓	✓		✓	✓

films. In the present work, only two molecules containing $-\text{SiMe}_3$ moiety (4, 6) have been identified in the gas phase in presence of ammonia, indicating that NH_3 could prevent the incorporation of methyl groups in the films.

Increasing the NH_3 flow rate from 20 sccm (Exp1) to 40 sccm (Exp2) does not modify the nitrogen content of the SiO_xN_y films, which remains at 6.2 at% N. This indicates either that the

nitrogen in the films is not linked to the concentration of NH_3 in the inlet gas, or that the latter is already saturated at 20 sccm NH_3 .

Removing ammonia from the gas phase (Exp3) yields surprising results. The nitrogen content slightly decreases, however the films still contain 5.8 at% N (Table 1). This indicates that the nitrogen in the films originates from TDMSA.

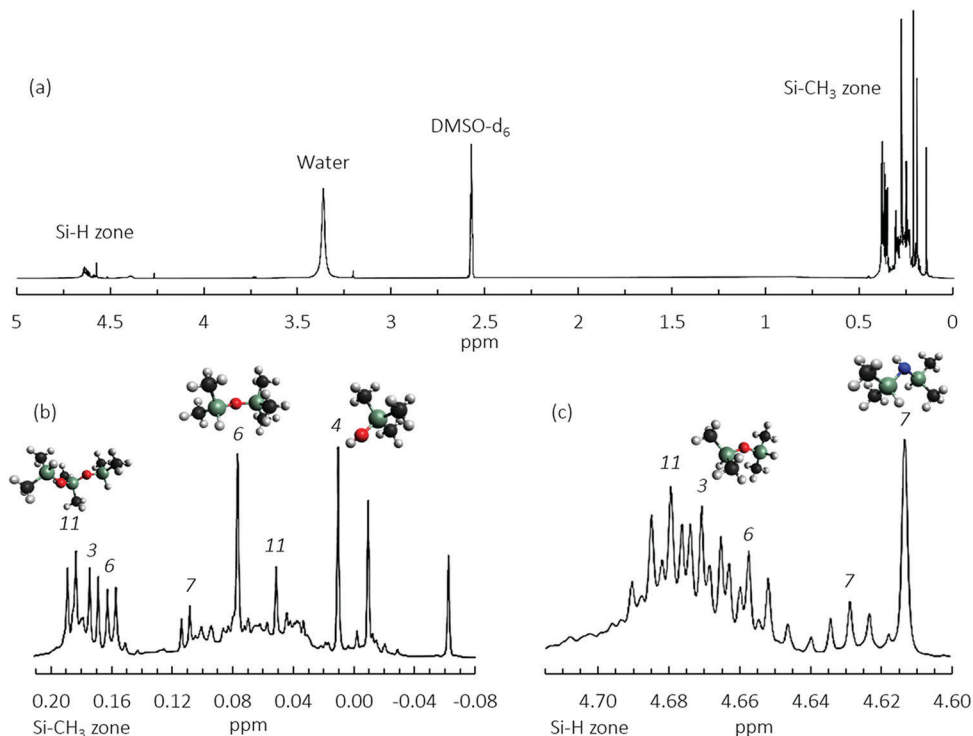


Fig. 2 NMR spectrum of Exp1 (a); zoom in the 4.60–4.72 ppm (b) and –0.01 to 0.22 ppm (c) range, 500 MHz in DMSO- d_6 .

It is concluded that dimethylsilylamine derivatives containing H-Si-N bonds, such as TDMSA, can be helpful in obtaining silicon oxynitride films at temperatures lower than 700 °C, without the requirement to add ammonia in the starting chemistry. This particular ability of such precursor molecules can be related to their molecular structure and is in agreement with results reported by Wrobel *et al.*,¹⁴ who highlighted that precursors lacking Si-H bonds in their structure are less reactive and require higher energies to overcome their activation step for Si₃N₄ or SiO_xN_y film formation. This renders molecules such as HMDSz less reactive than TDMSA, since the latter contains three Si-H bonds and the former none. In a similar context, Tomar *et al.*³⁹ reported that the Si₃N₄ deposition from HMDSz at 780 °C requires ammonia as a nitrogen source, in contrast to the present work, where SiO_xN_y films were formed from TDMSA in absence of NH₃ and at lower temperatures. In addition, both the precursor conversion percent and the average deposition rate remain unchanged, regardless of the presence or not of NH₃ in the inlet gas for similar O₂ flow rate and deposition temperature. In contrast, the carbon content of the films significantly increases under an ammonia-free atmosphere, suggesting that the key role of ammonia in the studied chemistry is to participate in the reduction of carbon incorporation in the film rather than to provide nitrogen, in agreement with previous works from Xia *et al.*⁴⁰ and Tijanic *et al.*⁴¹ among others. The increase of the carbon content (from 8.0 to 10.7 at%) and the slight decrease of nitrogen content (from 6.3 to 5.8 at%) in absence of NH₃ (Exp3) could therefore be linked to the larger number of compounds formed in Exp3, compared to Exp1 where NH₃ is present. As shown in Table 2, in addition to the

compounds previously observed in Exp1 (presence of NH₃), new by-products methoxytrimethylsilane MeOTMS (2), dimethylsilylanediol (5) and the silanamines PMDSz (8) and (13) are observed for Exp3. Among these, compounds 2, 4, 6 and 8 are trimethylsilane derivatives, which could be held accountable for the higher carbon content in the film. This is in coherence with Xia *et al.*,⁴⁰ who reported that reduction of carbon incorporation in silicon nitride or silicon oxynitride films depends on the use of dimethylsilane derivative precursors instead of trimethylsilyl ones.

With 40 sccm of ammonia (Exp2), a further decrease in carbon content is observed (5.9 at% C) whereas the nitrogen content is similar to Exp1. The relatively low and stable nitrogen incorporation under the various NH₃ flow rates confirms that NH₃ does not participate in enriching the films with nitrogen. Fewer by-products are observed for Exp2, with only compounds 1, 3, 4, 9, 11, 14 and 15 being identified. Among these molecules, only 4 is a SiMe₃-containing derivative, which correlates well with the overall lower carbon content in the films in comparison to Exp1 and Exp3. It is therefore evident that higher NH₃ flow rates reduce the number of by-products and more importantly results in fewer trimethylsilyl compounds in the gas phase and consequently, leads to films with lower carbon content. However, no enrichment in nitrogen is observed. As such, the non-requirement of NH₃ as a nitrogen source is highlighted, in chemistries where a silicon and nitrogen-containing molecule such as TDMSA is used as the precursor. This allows the chemical system to be simplified and utilize the combination of only O₂ as oxidant and TDMSA, with the latter fulfilling the dual role of silicon and nitrogen provider. Moreover, SiO_xN_y,

deposition is enabled at 650 °C thanks to the presence of Si-H bonds in the starting molecule.

3.2.2. Influence of the O₂ flow rate in absence of NH₃. The impact of the O₂ flow rate on the chemical composition of the deposited films as well as on the gas phase is studied for O₂ flow rates of 0.3 (Exp4) and 1.2 sccm (Exp5) and is compared to the reference experiment Exp3 with 0.6 sccm O₂ (Tables 1 and 2). As expected, when the O₂ flow rate is decreased from 0.6 to 0.3 sccm, the deposition rate of SiO_xN_y decreases from 1.6×10^{-3} to 1.0×10^{-3} mg min⁻¹. This decrease can be explained by the decrease of oxygen atoms available in the reactive gas phase. At the same time, the nitrogen content of the films increases from 5.8 at% (Exp3) to 9.8 at% (Exp4), indicating the more pronounced nitride character of the material. These results on the solid phase are a reflection of the changes induced in the gas phase. The decrease of the O₂ concentration in the input gas affects the global gas phase composition, with a decrease in the number of by-products observed by NMR and GC-MS (Table 2). For the lower O₂ flow rate (Exp4), dimethylsilanediol **5**, disiloxanes **6** and **9** and silanamines **13** and **15** are not detected, their absence being attributed to the lower oxygen flow rate. Naturally, a lower oxygen concentration in the gas phase translates to less oxidation of Si-C or Si-N bonds, which in turn are then free to participate in the formation of disilazanes TMSz (**7**) and HMDSz (**10**) and the silanamine PMDSz (**8**). Consequently, the presence of these compounds in the gas phase explains the higher nitrogen and carbon content of the films, given that they contain N-SiMe₂ and/or N-SiMe₃ moieties.

On the contrary, when the oxygen flow rate is increased from 0.6 to 1.2 sccm across Exp3 and Exp5, respectively, the opposite trend can be observed regarding the deposition rate and the N and C contents of the films (Table 1). Firstly, the higher O₂ flow in Exp5 results in a higher deposition rate, as expected. In terms of gaseous by-products, increase of O₂ supply facilitates the oxidation of Si-N or Si-C bonds and results in fewer nitrogen containing compounds compared to Exp3 and Exp4. The compounds identified for Exp5 are silanol **4**, methoxytrimethylsilane **2**, disiloxane **3**, disilazane **7**, trisiloxanes **11** and **12**, silanamines **13** and **15** (Table 2). Compounds **13** and **15**, composed of a -Si-N-Si-O-Si bonding sequence, seem to be convenient intermediary compounds for the formation of the SiO_xN_y film.

In summary, variation of the O₂ flow rate affects the nitrogen percentage in the film as follows: increase of the O₂ flow rate leads to the production of multiple siloxane products in the gas phase, which in turn readily participate in the formation of a -Si-O-Si- environment. The oxide character of the films is increased and the nitrogen content decreases in relation to it. This is also a consequence of the lower amount of nitrogen-containing silanamine compounds in the gas phase. In the same way, by reducing the O₂ flow rate, the formed film has a higher nitrogen content, which is also reflected in the presence of additional nitrogen-containing gaseous by-products.

An interesting point of observation is that for all experiments performed at 650 °C, the TDMSA conversion remains at around 81%. This could hint that oxygen is not participating in the

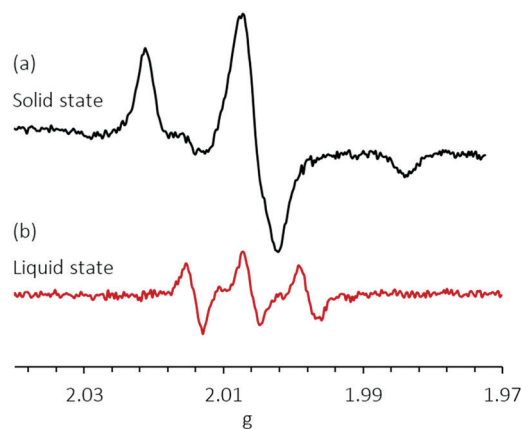


Fig. 3 ESR spectra of POBN-R* (Exp3) at the solid (a) and liquid (b) state.

activation of TDMSA, and that the temperature seems to be the main parameter influencing the TDMSA conversion.

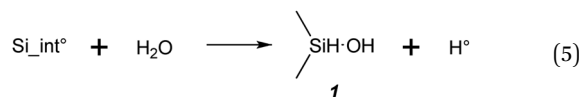
3.2.3. Depositions at 625 °C. An experiment at 625 °C has been undertaken (Exp6), exploring the possibility to further decrease the temperature of the thermal CVD process and to investigate the resulting gas phase. Based on the thermal behavior of TDMSA (Fig. 1), a conversion of approximately 40% is expected in absence of O₂ at this temperature. Interestingly, the addition of 0.6 sccm of O₂ in Exp6 results in a conversion of around 59%. Both conversion percentages are lower than the one noted at 650 °C. However, it is important to underline that at 625 °C, an oxygenated atmosphere leads to a higher conversion of TDMSA. As a conclusion, for the adopted process conditions, the temperature is the only parameter that has an impact on the precursor conversion at 650 °C, whereas at 625 °C addition of oxygen increases it. The participation of oxygen in the precursor conversion at lower temperature hints at a potentially different reaction pathway compared to the one followed at 650 °C.

Regarding the average deposition rate and the N and C content of the films, all values were noted to decrease when the temperature was lowered from 650 °C (Exp3) to 625 °C (Exp6). This is a direct consequence of the lower precursor conversion percent at 625 °C, which also influences the gas phase composition. Fewer by-products (**4**, **7**, **9**, **11-15**) are observed at 625 °C, as a result of two potential reasons. The lower conversion of the precursor results in a lower concentration of species that would otherwise act as the building blocks for the formation of additional by-products, and/or it is not possible to form the latter due to the decrease in supplied energy (*i.e.* lower deposition temperature).

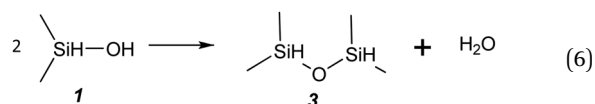
3.3. Mechanistic investigation

3.3.1. ESR study of radical intermediates. ESR study was performed in order to gain further insight into the deposition mechanism. In order to observe reactive species such as radicals, a spin-trap molecule was encapsulated in a KBr pellet. The advantages of this methodology are, first, the encapsulation offers thermal protection of the organic spin-trap molecule, and second, it helps avoid dispersion of the spin-trap powder within the reactor. A spin-trap, with a decomposition

is at 250 °C. In an alternative route, H• could form water with O₂, which will in turn react with Si_{int}• to form compound 1, eqn (5), although it is considered that this reaction is taking place at slower rates.

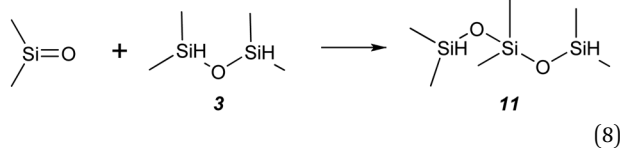
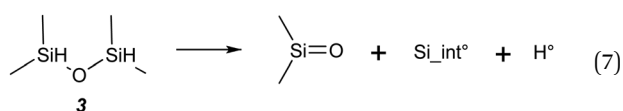


Reaction of the silanol compound 1 with an oxygen radical can lead to the production of the silanediol compound 5, as shown in eqn (4). Moreover, the condensation of two silanol molecules, 1, produced according to eqn (4) or eqn (5), can then result in the formation of compound 3, eqn (6).



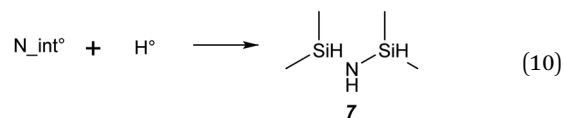
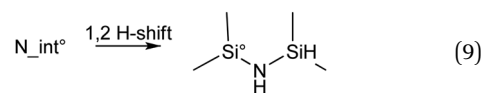
As suggested by Pola *et al.*,⁴⁶ siloxane molecules can disproportionate into a silanone and a radical species when given enough energy, with the radical species participating in the polymerization of other siloxane molecules. Following this proposition, compound 3 is assumed to yield Si_{int}•, H• and a dimethylsilanone through eqn (7). The radical species H• and Si_{int}• can additionally react together to form dimethylsilane. This compound is not observed in the gas phase; however, it is highly reactive and can be potentially formed and consumed very rapidly. Moreover, being in an oxidizing atmosphere, dimethylsilane could be oxidized into silanol compounds such as 1 and 5. The newly formed silanols can in turn participate in the formation of 3 through eqn (6), producing a continuous cycle between eqn (4) and/or eqn (5) with eqn (6) and (7).

The silanone formed through eqn (7) is then used to polymerize TMDSO 3 into HMDSO 11 through eqn (8).

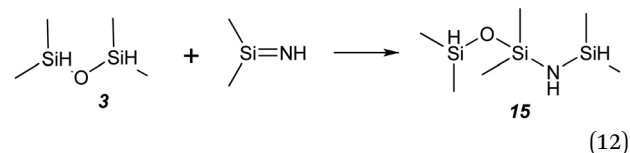
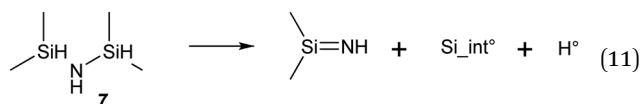


It is recalled that decomposition of TDMSA through eqn (1) also yields N_{int}•. This radical compound can undergo a 1,2 H-shift, yielding a new Si-centered radical,³⁵ eqn (9), or it can react with a H• leading to the formation of TMDSz 7, eqn (10). All of the detected nitrogen-containing by-products (Table 2) feature a hydrogenated nitrogen atom, further supporting the 1,2 H-shift. Moreover, the formation of the new Si-centered radical through this 1,2 H-shift could in fact explain why only Si-centered species are identified by ESR, despite eqn (1)

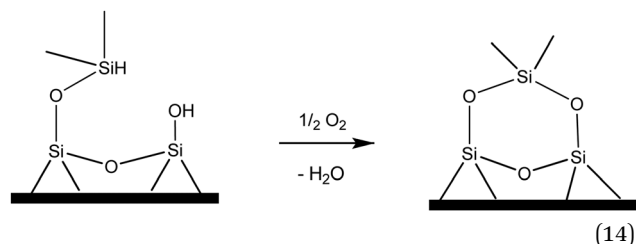
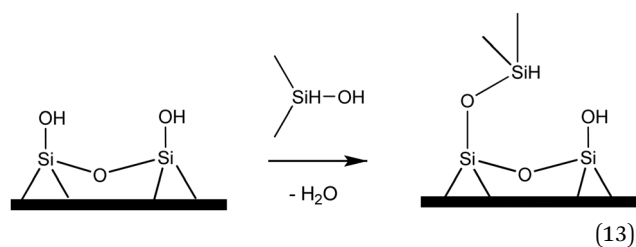
yielding two different radical species (Si_{int}• and N_{int}•).



Following the same reasoning as for TMDSO 3, TMDSz 7 can also disproportionate and yield Si_{int}•, H• and a silanimine, eqn (11), which can in turn be used to polymerize siloxanes and drive the formation of bi-functional compounds with a -Si-N-Si-O-Si- sequence such as 15, eqn (12). The presence of 15 in the gas phase even in absence of NH₃, emphasizes the participation of TDMSA in the formation of silicon oxynitride films.

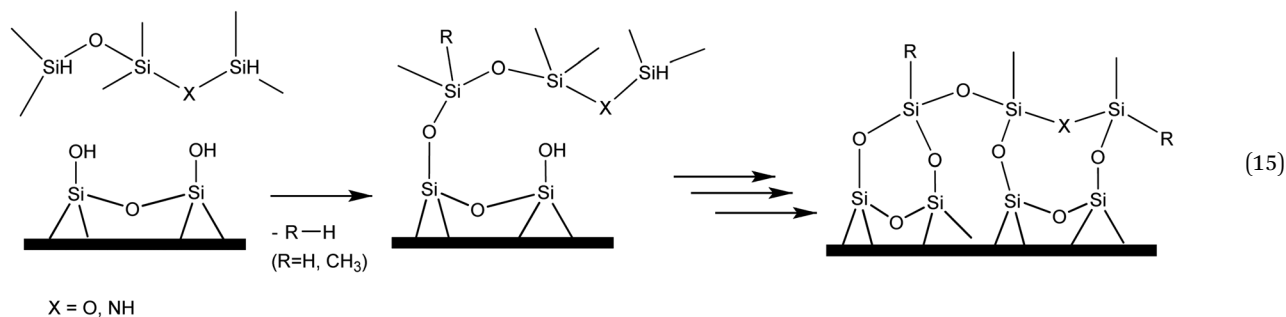


Film formation. Si_{int}• is present in the gas phase in large concentrations, produced from eqn (1), (7) and (11). Thus, it can be involved in the formation silica-type film by reacting with the silanol sites of the substrate surface, as illustrated in eqn (13) and (14). The siloxane formed in eqn (13), can then be oxidized by oxygen from the gas phase before reacting with the geminal silanol on the substrate, eqn (14).



The low amount of nitrogen in the film suggests a major incorporation of oxygen with siloxane compounds 3, 6 and 12, eqn (13) and (14), while the incorporation of nitrogen itself is

only possible through a few molecules such as **13** and **15**. In eqn (15), a general mechanism for the formation of SiO_xN_y film from trisiloxane **11** ($\text{X}=\text{O}$) and silanamine **15** ($\text{X}=\text{NH}$) is proposed. The adsorption and oxidation mechanism of these molecules from the gas phase onto the substrate is similar to eqn (13) and (14), but will result in the formation of a silicon oxynitride film in the case of molecules such as **15**, containing a Si-N-Si-O-Si- sequence, eqn (15). The first step when **15** is reacting with the substrate is the formation of an O-Si bond (stronger than a N-Si one), which can act as the driving force of the deposition mechanism.



The proposed simplified mechanism paves the way to the kinetic numerical modelling of the studied TDMSA- O_2 CVD process. The aim of modelling such systems is (i) the optimization of the deposition conditions and of the reactor geometry to uniformly treat various substrates, whether they are planar or more complex and to reach target film thickness and composition, (ii) to help the process scale up.

4. Conclusion

Simultaneous analysis of the gas phase during the atmospheric pressure CVD (APCVD) of silicon oxynitride from tris(dimethylsilyl)amine (TDMSA) involving chemistries was carried out, using a combined GC-MS, ESR and NMR investigation. This novel methodology, implemented for the first time in a SiO_xN_y thermal CVD process, allows understanding the impact of the molecular structure of the starting silane precursor on the operating conditions and the stoichiometry of the formed film. The combined detailed analysis by GC-MS and NMR highlighted the wealth of the gas phase chemistry and its evolution as a function of the investigated process conditions.

Through quantitative GC-MS analysis, it was found that the TDMSA precursor decomposes in the 580–700 °C range in absence of oxygen. For temperatures higher than 650 °C, decomposition of the precursor is purely temperature-driven, but for lower temperatures, a higher conversion is observed upon the addition of O_2 .

The overall molecular structure of the precursor and the multiple potential decomposition pathways underlie the complexity of the gas phase, giving rise to a large number of gaseous by-products. Variation of the operating conditions lead to the detection of up to 15 compounds in the gas phase and the

production of films with varying compositions. An increase of the O_2 flow rate leads to the production of multiple siloxane compounds in the gas phase, which was reflected in a more pronounced oxide character of the SiO_xN_y films. In contrast, by reducing the O_2 flow rate, additional nitrogen-containing gaseous by-products were detected in the gas-phase and the deposited film has a higher nitrogen content. Interestingly, fewer by-products were detected when NH_3 was added in the inlet chemistry, including absence of trimethylsilane derivatives, which was proposed to be the reason for the lower carbon impurities found in the SiO_xN_y films under NH_3 flow.

A significant result was the deposition of silicon oxynitride films even in absence of ammonia, demonstrating the judicious choice of the TDMSA silanamine as a dual source of nitrogen and silicon. No synergetic effect of ammonia addition in the TDMSA- O_2 system was observed in terms of nitrogen content modulation for the tested operating conditions. Additionally, the presence of Si-H bonds in the precursor structure renders it possible to form SiO_xN_y films by thermal CVD, at temperatures lower than those required by other conventional silazane/silanamine precursors such as HMDSz. As a result, it is demonstrated that the TDMSA precursor, or molecules with a similar structure (presence of N-Si-H bonds), can open the way to new developments of silicon oxynitride deposition processes without requiring NH_3 , thus simplifying system complexity.

Finally, the combined study of the gas phase using GC-MS, NMR and ESR provided valuable insight in the deposition mechanism. The decomposition of the TDMSA precursor through a homolytic cleavage of its Si-N bond was narrowed down through the detection of a silylated $\text{Me}_2\text{HSi}^\bullet$ radical by ESR. Consideration of the decomposition pathways and the by-products identified in the gas phase allowed the proposal of multiple potential reactions highlighting the mechanisms involved in the solid film formation. These results open the way to develop a kinetic numerical model of the CVD process aiming to find optimized deposition conditions or reactor geometries to uniformly coat planar or more complex-in-shape substrates for targeted applications. The methodology developed in this work to characterize both stable compounds as well as radical species in the reactor effluents can be applied to other chemical systems, in the vision of CVD process development and optimisation.

Abbreviations

TDMSA	Tris(dimethylsilyl)amine
HMDSz	Hexamethyldisilazane
BTBAS	Di("butylamino)silane
APMDES	3-Aminopropylmethyl-diethoxysilane
TEOS	Tetraethoxysilane
TMDSz	1,1,3,3-Tetramethyldisilazane
TDMAS	Tris(dimethylamino)silane
PMDSz	Pentamethyldisilazanes
MeOTMS	Methoxytrimethylsilane
TMDSO	1,1,3,3-Tetramethyldisiloxane
PMDSO	Pentamethyldisiloxane
HMTSO	Hexamethyltrisiloxane
HMCTSO	Hexamethylcyclotrisiloxane
POBN	α -(4-Pyridyl-1-oxide)- <i>N</i> - <i>tert</i> -butylnitron

Conflicts of interest

The authors declare no conflicts of interest.

Acknowledgements

The present work was funded by the French Agence Nationale de la Recherche (ANR) under the Contract HEALTHYGLASS ANR-17-CE08-0056. The authors are indebted to Lionel Rechinat, LCC UPR, and Eric Leroy, ICT, for fruitful discussions on ESR and GC-MS analyses respectively. Anonymous reviewers are also acknowledged for their constructive comments and suggestions.

References

- 1 Y. Shi, L. He, F. Guang, L. Li, Z. Xin and R. Liu, A review: preparation, performance, and applications of silicon oxynitride film, *Micromachines*, 2019, **10**, 552.
- 2 M. Shahpanah, S. Mehrabian, M. Abbasi-Firouzjah and B. Shokri, Improving the oxygen barrier properties of PET polymer by radio frequency plasma-polymerized SiO_xN_y thin film, *Surf. Coat. Technol.*, 2019, **358**, 91–97.
- 3 Z. Zhang, Z. Shao, Y. Luo, P. An, M. Zhang and C. Xu, Hydrophobic, transparent and hard silicon oxynitride coating from perhydropolysilazane, *Polym. Int.*, 2015, **64**, 971–978.
- 4 Y. Shima, H. Hasuyama, T. Kondoh, Y. Imaoka, T. Watari and K. Baba, *et al.*, Mechanical properties of silicon oxynitride thin films prepared by low energy ion beam assisted deposition, *Nucl. Instrum. Methods Phys. Res., Sect. B*, 1999, **148**, 599–603.
- 5 E. K. Park, S. Kim, J. Heo and H. J. Kim, Electrical evaluation of crack generation in SiN_x and SiO_xN_y thin-film encapsulation layers for OLED displays, *Appl. Surf. Sci.*, 2016, **370**, 126–130.
- 6 P. Temple-Boyer, B. Hajji, J. Alay, J. Morante and A. Martinez, Properties of SiO_xN_y films deposited by LPCVD from SiH₄/N₂O/NH₃ gaseous mixture, *Sens. Actuators, A*, 1999, **74**, 52–55.
- 7 M. J. Rand and J. F. Roberts, Silicon Oxynitride Films from the NO-NH 3-SiH₄ Reaction, *J. Electrochem. Soc.*, 1973, **120**, 446.
- 8 J. Steffens, M. A. Fazio, D. Cavalcoli and B. Terheiden, Multi-characterization study of interface passivation quality of amorphous sub-stoichiometric silicon oxide and silicon oxynitride layers for photovoltaic applications, *Sol. Energy Mater. Sol. Cells*, 2018, **187**, 104–112.
- 9 G. Kovačević and B. Pivac, Reactions in silicon–nitrogen plasma, *Phys. Chem. Chem. Phys.*, 2017, **19**, 3826–3836.
- 10 N. I. Fainer, A. G. Plekhanov, M. N. Khomyakov, E. A. Maksimovskiy and Y. M. Rumyantsev, The influence of the conditions of synthesis on the composition and mechanical properties of silicon oxycarbonitride nanocomposite films, *Prot. Met. Phys. Chem. Surf.*, 2017, **53**, 253–260.
- 11 T. Otani and M. Hirata, High rate deposition of silicon nitride films by APCVD, *Thin Solid Films*, 2003, **442**, 44–47.
- 12 N. Bahlawane, K. Kohse-Höinghaus, P. A. Premkumar and D. Lenoble, Advances in the deposition chemistry of metal-containing thin films using gas phase processes, *Chem. Sci.*, 2012, **3**, 929–941.
- 13 V. Tomar, D. Patil and D. Gautam, Deposition and characterization of SiON films using HMDS for photonics applications, *Semicond. Sci. Technol.*, 2006, **22**, 43.
- 14 A. M. Wrobel, A. Walkiewicz-Pietrzykowska and I. Blaszczyk-Lezak, Reactivity of organosilicon precursors in remote hydrogen microwave plasma chemical vapor deposition of silicon carbide and silicon carbonitride thin-film coatings, *Appl. Organomet. Chem.*, 2010, **24**, 201–207.
- 15 J. W. Smith, S. M. Seutter and R. S. Iyer, Thermal Chemical Vapor Deposition of Bis (Tertiary-Butylamino) Silane-based Silicon Nitride Thin Films: Equipment Design and Process Optimization, *J. Electrochem. Soc.*, 2005, **152**, G316.
- 16 J. Gumphier, W. Bather, N. Mehta and D. Wedel, Characterization of low-temperature silicon nitride LPCVD from bis (tertiary-butylamino) silane and ammonia, *J. Electrochem. Soc.*, 2004, **151**, G353.
- 17 H. M. Park, J. Y. Lee, K. Y. Jee, S.-I. Nakao and Y. T. Lee, Hydrocarbon separation properties of a CVD-deposited ceramic membrane under single gases and binary mixed gas, *Sep. Purif. Technol.*, 2021, **254**, 117642.
- 18 V. E. Vamvakas, R. Berjoan, S. Schamm, D. Davazoglou and C. Vahlas, Low pressure chemical vapor deposition of silicon oxynitride films using tetraethylorthosilicate, dichlorosilane and ammonia mixtures, *J. Phys. IV*, 2001, **11**, Pr3-P231–Pr233-238.
- 19 E. Halova, S. Alexandrova, A. Szekeres and M. Modreanu, LPCVD-silicon oxynitride films: interface properties, *Microelectron. Reliab.*, 2005, **45**, 982–985.
- 20 B. Kaghouché, F. Mansour, C. Mollet, B. Rousset and P. Temple-Boyer, Investigation on optical and physico-chemical properties of LPCVD SiO_xN_y thin films, *Eur. Phys. J.: Appl. Phys.*, 2014, **66**, 20301.
- 21 S. Alexandrov, A. Kovalgin and D. Krasovitskiy, A study of CVD of gallium nitride films by in situ gas-phase UV spectroscopy, *J. Phys. IV*, 1995, **5**, C5-C183–C185-190.

- 22 K. Kachel, D. Siche, S. Golka, P. Sennikov and M. Bickermann, FTIR exhaust gas analysis of GaN pseudohalide vapor phase growth, *Mater. Chem. Phys.*, 2016, **177**, 12–18.
- 23 T. Ohba, T. Suzuki, H. Yagi, Y. Furumura and T. Hatano, Decomposition property of methylhydrazine with titanium nitridation at low temperature, *J. Electrochem. Soc.*, 1995, **142**, 934.
- 24 M. M. Nolan, S. Y. Kim, A. Koley, T. Anderson and L. McElwee-White, *In Situ* Investigation of the Thermal Decomposition of $\text{Cl}_4(\text{CH}_3\text{CN})\text{W}(\text{NiPr})$ During Simulated Chemical Vapor Deposition, *Eur. J. Inorg. Chem.*, 2019, 3661–3666.
- 25 F. Lloret, K. J. Sankaran, J. Millan-Barba, D. Desta, R. Rouzbahani and P. Pobedinskas, *et al.*, Improved Field Electron Emission Properties of Phosphorus and Nitrogen Co-Doped Nanocrystalline Diamond Films, *Nanomaterials*, 2020, **10**, 1024.
- 26 W. G. Zhang and K. J. Hüttinger, CVD of SiC from methyltrichlorosilane. Part II: Composition of the gas phase and the deposit, *Chem. Vap. Deposition*, 2001, **7**, 173–181.
- 27 J. Arnó, Z. Yuan and S. Murphy, Fourier Transform Infrared Characterization of Downstream Gas-Phase Species Generated by Tetraethylorthosilicate/Ozone Atmospheric Pressure Reactions, *J. Electrochem. Soc.*, 1999, **146**, 276–280.
- 28 M. Yoshimoto, K. Takubo, M. Komoda and H. Matsunami, Gas phase reactions diagnosed by mass analysis in photo-assisted chemical vapor deposition of silicon nitride, *Appl. Surf. Sci.*, 1994, **79**, 264–269.
- 29 T. Sorita, T. Satake, H. Adachi, T. Ogata and K. Kobayashi, Mass Spectrometric and Kinetic Study of Low-Pressure Chemical Vapor Deposition of Si_3N_4 Thin Films from SiH_2Cl_2 and NH_3 , *J. Electrochem. Soc.*, 1994, **141**, 3505.
- 30 N. I. Fainer, A. G. Plekhanov, A. N. Golubenko, Y. M. Rumyantsev, E. A. Maksimovskii and V. R. Shayapov, Structure and elemental composition of transparent nanocomposite silicon oxycarbonitride films, *J. Struct. Chem.*, 2017, **58**, 119–125.
- 31 H. Pedersen, Time as the Fourth Dimension: Opening up New Possibilities in Chemical Vapor Deposition, *Chem. Mater.*, 2016, **28**, 691–699.
- 32 D. K. Russell, I. M. Davidson, A. M. Ellis, G. P. Mills, M. Pennington and I. M. Povey, *et al.*, The kinetics and mechanism of the pyrolysis of manganese and manganese silicide CVD precursors, *Chem. Vap. Deposition*, 1998, **4**, 103–107.
- 33 K. C. Topka, G. A. Chliavoras, F. Senocq, H. Vergnes, D. Samelot and D. Sadowski, *et al.*, Large temperature range model for the atmospheric pressure chemical vapor deposition of silicon dioxide films on thermosensitive substrates, *Chem. Eng. Res. Des.*, 2020, **161**, 146–158.
- 34 M. D. Hanwell, D. E. Curtis, D. C. Lonie, T. Vandermeersch, E. Zurek and G. R. Hutchison, Avogadro: an advanced semantic chemical editor, visualization, and analysis platform, *J. Cheminf.*, 2012, **4**, 17.
- 35 W. Knolle, L. Wennrich, S. Naumov, K. Czihal, L. Prager and D. Decker, *et al.*, 222 nm Photo-induced radical reactions in silazanes. A combined laser photolysis, EPR, GC-MS and QC Study, *Phys. Chem. Chem. Phys.*, 2010, **12**, 2380–2391.
- 36 R. Pandey, L. Patil, J. Bange, D. Patil, A. Mahajan and D. Patil, *et al.*, Growth and characterization of SiON thin films by using thermal-CVD machine, *Opt. Mater.*, 2004, **25**, 1–7.
- 37 J. H. Lee, C. H. Jeong, J. T. Lim, V. A. Zavaleyev, S. J. Kyung and G. Y. Yeom, SiO_xN_y thin film deposited by plasma enhanced chemical vapor deposition at low temperature using HMDS- O_2 - NH_3 -Ar gas mixtures, *Surf. Coat. Technol.*, 2007, **201**, 4957–4960.
- 38 R. González-Luna, M. Rodrigo, C. Jiménez and J. Martínez-Duart, Deposition of silicon oxinitride films from hexamethyldisilazane (HMDS) by PECVD, *Thin Solid Films*, 1998, **317**, 347–350.
- 39 V. Tomar, L. Patil and D. Gautam, Deposition and characterization of silicon nitride films using HMDS for photonics applications, *J. Optoelectron. Adv. Mater.*, 2008, **10**, 2657–2662.
- 40 B. Xia, M. L. Fisher, H. Stemper and A. Misra, One-step growth of HfSiON films, *Thin Solid Films*, 2008, **516**, 5460–5464.
- 41 Z. Tijić, D. Ristić, M. Ivanda, I. Bogdanović-Radović, M. Marčuš and M. Ristić, *et al.*, Low Temperature Deposition of SiN_x Thin Films by the LPCVD Method, *Croat. Chem. Acta*, 2012, **85**, 97–100.
- 42 L. Gorla-Gatti, A. Iannone, A. Tomasi, G. Poli and E. Albano, In vitro and in vivo evidence for the formation of methyl radical from procarbazine: a spin-trapping study, *Carcinogenesis*, 1992, **13**, 799–805.
- 43 A. J. Carmichael, K. Makino and P. Riesz, Quantitative aspects of ESR and spin trapping of hydroxyl radicals and hydrogen atoms in gamma-irradiated aqueous solutions, *Radiat. Res.*, 1984, **100**, 222–234.
- 44 H. Chandra, I. M. Davidson and M. C. Symons, Unstable intermediates. Part 202. The use of spin traps to study trialkylsilyl and related radicals, *J. Chem. Soc., Perkin Trans. 2*, 1982, 1353–1356.
- 45 H. Chandra, I. M. T. Davidson and M. C. R. Symons, Use of spin traps in the study of silyl radicals in the gas phase, *J. Chem. Soc., Faraday Trans. 1*, 1983, **79**, 2705–2711.
- 46 J. Pola, A. Galíková, A. Galík, V. Blechta, Z. Bastl and J. Šubrt, *et al.*, UV Laser Photolysis of Disiloxanes for Chemical Vapor Deposition of Nano-Textured Silicones, *Chem. Mater.*, 2002, **14**, 144–153.